PHYSICAL REVIEW B **69**, 041405(R) (2004)

Evidence for interstitial hydrogen as the dominant electronic defect in nanometer alumina films

D. R. Jennison,* P. A. Schultz, and J. P. Sullivan
Sandia National Laboratories, Albuquerque, New Mexico 87185-1415, USA
(Received 9 July 2003; published 28 January 2004)

We provide experimental and first principles theoretical evidence that electron transport through alumina films on Al(111) occurs through electron tunneling mediated by interstitial (i.e., nonbonded) H defects within the 6-nm amorphous surface oxide. Experiments indicate field-assisted tunneling into a defect level near midgap in the oxide and conductance that increases with increasing H content. Using density functional theory, we find interstitial neutral H indeed produces a midgap trap. Moreover, with a negatively charged H, the full $1s^2$ orbital is almost at the *same* mid-gap energy. This shows H^- electron-electron interactions are well screened in this wide gap insulator and can mediate conduction.

DOI: 10.1103/PhysRevB.69.041405 PACS number(s): 73.50.−h, 71.15.Mb, 73.40.Rw

Electronic conduction through ultrathin films of alumina is important for a number of electronic devices, including superconducting Josephson junctions,[1] single electron transistors, and magnetic tunnel junctions.[2,3] In addition, electronic conductance limits the thickness of the alumina layer that forms on aluminum metal when exposed to air or O_2(g) and limits the rate of electrochemical cathodic processes when Al is immersed in aqueous solutions. These latter processes influence the effectiveness of alumina as a passivating film on Al, critical for the corrosion resistance of the metal.[4]

Despite the importance of electronic conduction in alumina, there is a limited knowledge of the dominant electronic defects that cause it. On the basis of ballistic electron emission microscopy (BEEM), it was suggested that electronic conduction is associated with disorder-related defect states that tail a few eV from the band edges to deep within the oxide gap.[5] Recently, however, it was shown electronic conductivity of an alumina film increases dramatically when immersed in H_2O.[6] Exposure to H_2O has been shown to increase the H content, as detected by elastic recoil detection,[7] (ERD) or secondary ion mass spectroscopy,[8] suggesting the involvement of H in creating electronic defects. Here we examine the role H plays in conductance in alumina films.

The experimental section describes transport vs temperature and film thickness, concluding that field-assisted or Fowler-Nordheim tunneling, which permits electrons to be injected into the film defect level, defines the mechanism. These electrons then move from defect to defect. The theoretical work was based on a bulk alumina structure determined from prior theory on this highly ionic material.[9–12] We used the κ-Al_2O_3 phase[9] with density functional theory (DFT) (Ref. 13) and both supercell bulk and slab models to (1) determine the neutral H location and the energy level with respect to κ-Al_2O_3 band edges; (2) determine the H^- $1s^2$ defect level, thus indicating the conduction electron energy; and (3) locate these levels with respect to the Fermi level (E_f) of the underlying Al metal. Our results strongly suggest that interstitial (i.e., nonbonded) H is responsible for both conduction through the alumina films and the experimental defect level.

The electronic conduction mechanism in alumina and the position of the dominant electronic defect level was made through current-voltage, current-temperature, and admittance-frequency measurements of variable thickness alumina films on Al metal. Samples with varying alumina thickness were prepared on vacuum evaporated thin films of Al and on single crystal Al disks polished to expose either the (111), (110), or (100) surface. The Al films, 0.15–0.2 μm thick, were deposited in high vacuum on SiO_2-coated Si wafers. Alumina layers of increasing thickness were formed by (1) exposing the Al surface to pure O_2(g) at 1 Torr for 90 min (O_2 formed), (2) oxidizing Al in an electron cyclotron resonance (ECR) oxygen plasma for 10 min (plasma oxidized), or (3) depositing alumina on top of Al using thermal evaporation of Al combined with ECR plasma oxidation (plasma deposited). Alumina films were prepared on the bulk single crystals by mechanical polishing of the disks using colloidal alumina polishing solutions followed by air oxidation, which results in an oxide thickness that varies with crystallographic orientation. All of the oxides formed in these procedures were amorphous, determined by transmission electron microscopy and diffraction.

Electrical measurements were taken by attaching Au probes to lithographically patterned Au contacts on the oxide surface, creating metal-insulator-metal capacitor structures. Electrical contact was made to the underlying Al and Au top electrodes using W and Au needle probes, respectively. Typical contact areas were 50×50 μm^2.

The mechanism of electron conduction in alumina is established through temperature-dependent and thickness-dependent conductance measurements. The activation energy for electron transport through the thin alumina films was found to be 0.04 eV,[7] indicating conduction is not thermally activated and is therefore not Schottky-emission or Frenkel-Poole conduction. Both rely on thermal activation of carriers over sizable activation barriers. The thickness dependence of the electron conductance definitively identifies the transport mechanism. Current through alumina films of different thicknesses is shown in Fig. 1. With exception of the plasma-oxidized sample, current decreases exponentially with the oxide thickness. The lack of thermal activation to the current, and the exponential dependence on the insulator thickness, indicates the electron transport in thin alumina films is limited by field-assisted or Fowler-Nordheim tunneling, with a current dependence given by

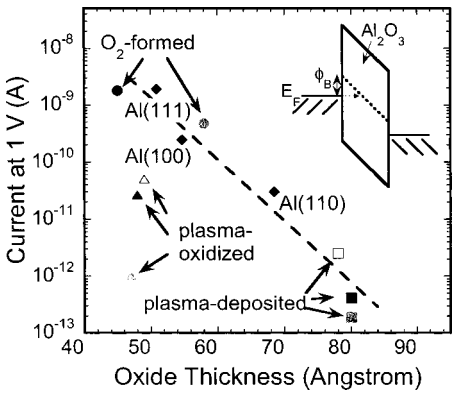

FIG. 1. Current vs oxide thickness for alumina films on thin film Al and bulk Al single crystals. Oxide thickness was determined through capacitance measurements of the metal-insulator-metal structures, assuming a dielectric constant of 8.0 for alumina. The dashed line is the best fit to the data, excluding the plasma-oxidized sample. For the thin film samples, the open symbols are the measured conductance following H_2O immersion of the film, and the gray symbols are the measured current following anodic electrochemical polarization of the Al. The inset schematically shows the field-assisted tunneling conduction process and the position of the electronic defect.

$$I \propto \left(\frac{V}{t}\right)^2 \exp\left[-\frac{4t\sqrt{2m^*}(q\phi_B)^{3/2}}{3q\hbar V}\right], \qquad (1)$$

where I is the measured current through the insulator, V the applied voltage, t the insulator thickness, m^* the carrier effective mass, and ϕ_B the barrier height for tunneling.[14]

Electronic conduction is limited by the rate at which carriers with energy E_f can be injected from the metal and tunnel through the triangular barrier into a defect level in the oxide (see Fig. 1, inset). For a sufficiently high defect density, carrier propagation through the remainder of the oxide occurs by trap-assisted tunneling, i.e., hopping between isolated defects (not rate limiting). The position of the defect level with respect to the metal E_f is given by the height of the tunneling barrier, ϕ_B, and determined from the slope of current vs thickness (the dashed line in Fig. 1). Excluding the plasma-oxidized sample, a least squares fit to the slope yields a value of 0.241 $Å^{-1}$, indicating ϕ_B, $\approx 0.50(m^*/m_e)^{1/3}$ V. Using BEEM measurements, Rippard *et al.* estimated $m^*/m_e \approx 0.75$ for thin alumina films.[5] This value would give $\phi_B = 0.45$ V, i.e., a defect level 0.45 eV above E_f.

Measured H concentrations in alumina films and changes in the electron conductance of the films following electrochemical treatment give evidence to H-related electronic defects. Plasma-oxidized alumina films exhibit a much lower H content (order of magnitude) than O_2-formed and plasma-deposited alumina films, as determined from ERD.[8] This coincides with much reduced electron conductance observed for these films. The H content in the oxide can be altered by an electrochemical treatment.[15] Thin film samples were immersed in 0.05-M K_2SO_4 solutions at open circuit (no applied potential) and at applied potentials that gave rise to 10 nA of anodic current (positive potential on the Al with respect to a counter electrode in solution) and 10 nA of cathodic current (negative potential on the Al). Immersion in H_2O at open circuit increases the H content of the oxide, as detected by ERD.[8] In Fig. 1, the effect of immersion (open symbols) and anodic polarization (gray symbols) is shown. H_2O immersion leads to an increased conductance, consistent with increased H content. The effect is most apparent for oxides that do not thicken upon immersion. In contrast, anodic polarization is expected to expel mobile positively charged defects, e.g., protons, from the film due to field-assisted diffusion away from the positively-charged Al metal. As shown in Fig. 1, anodic polarization leads to a reduced conductance, consistent with a reduced H content. Hence, we conclude conduction does indeed involve H.

As stated above, the Al metal surface, exposed to ambient conditions, develops a thin amorphous oxide. To model this surface film, we use the κ-Al_2O_3 phase. κ-Al_2O_3 has a very similar density to amorphous alumina and is more representative of the film than the more stable, but significantly more dense, sapphire (α-Al_2O_3) phase. The atomic structure of κ-Al_2O_3 has recently been established.[9] Like sapphire (and other lower temperature phases such as γ- or θ-Al_2O_3) it is highly ionic,[10] with Al^{3+} ions arranged about an otherwise close packed array of O^{2-} ions. In sapphire, all Al ions are in octahedral sites and the planes are only minimally buckled. The κ phase has $\frac{3}{4}$ octahedral and $\frac{1}{4}$ tetrahedral Al ions and significant buckling occurs in the planes of O ions.[9] This produces large empty regions within the crystal. In the surface film (in the absence of an OH containing phase), the amorphous character is likely due to a lack of long range order in the Al-ion sublattice.[12] We suggest that similar properties in the amorphous material result in an easy penetration of neutral H.[7,8]

Our slab density functional theory (DFT) calculations used the Vienna *ab initio* Simulations Package (VASP) (Ref. 16) in the local density approximation (LDA) (Ref. 17) and the generalized gradient approximation (GGA) known as PW91.[18] The ultrasoft pseudopotentials of Vanderbilt[19] describe the κ-Al_2O_3 system to high accuracy with a plane wave cutoff of 270 eV. However, a higher cutoff of 396 eV is needed if covalent oxygen, such as the OH at the oxide surface, is present. Eigenvalues from LDA vs GGA differ negligibly. Structural energy minimization used a damped molecular dynamics algorithm, and geometries were considered relaxed when residual forces were less than 0.03 eV/Å. Tests showed that 6 **k** points converge to 0.02 eV in total energy. Because of long-range electrostatic forces in ionic systems, we used a large vacuum gap between the VASP slabs. We found 15 Å separation or greater to be adequate.

Calculations were done with an κ-Al_2O_3 slab consisting of five O layers on top of a four-layer slab of Al(111). The closest packed κ-Al_2O_3 planes were used on the outer surfaces of the oxide layer, in an *A*-*B*-*A*-*C*-*A* stacking in the notation of Yourdshahyan *et al.*[9] Since the native surface oxide is terminated by OH,[20] we altered the top layer in the manner of sapphire(0001),[20] removing 1 ML of O ions and $\frac{1}{3}$ ML of near-surface Al ions, and replacing both with 1 ML of OH. This preserves the *A*-plane unit cell charge of -3 so the deeper planes are minimally disturbed, as in sapphire.[20] First the oxide and metal slabs were relaxed separately. Then the

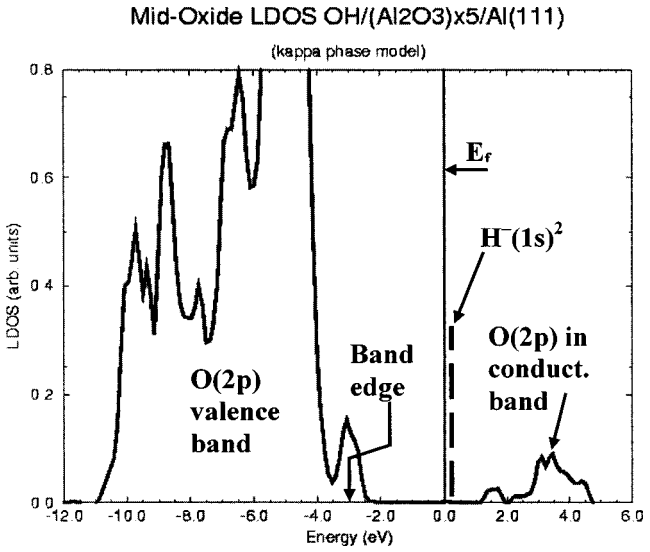

FIG. 2. The mid-plane O local density of states for the κ-Al_2O_3 film on Al(111). The position of the conduction electron, found from the calculation of the interstitial H^-, is indicated by the dashed line and is roughly 0.2 eV above the Al metal Fermi level (E_f). The conduction band has very little O character because of the high ionicity in this material (see Ref. 10). Though the O(2p) valence band edge is obscured by the remnant of the interface, its estimated position is shown.

two fixed slabs were brought together until the inter-slab energy was minimized. Finally a full relaxation was performed, with the bottom two Al metal layers frozen at the GGA bulk distance.

One possibility is that H-related conductivity stems from OH in the alumina layer. However, the OH ion has a large energy difference between the highest filled lone-pair orbital and the lowest empty orbital (σ^*). The antibonding σ^* is therefore unlikely to be responsible for conductivity. Placing OH on the surface, we observed the energy positions of the highest occupied and σ^* OH levels. We find these lie outside (though near) the edges of the film band gap. When the film is on Al metal, they are far from the E_f, which we find to be in the middle of the oxide band gap.

Both surface (the σ^*) and interface states exist close to the band edges. The latter may be what Ruberto *et al.*[21] observed in studying possible cleavage surfaces in κ-Al_2O_3. They found a partially filled metallic state regardless of how the crystal was cleaved. Here the interface state is well below the Al E_f and completely filled. In the local density of states (LDOS) of the O ions, the amplitudes fall exponentially towards the center of the oxide slab from either direction. Figure 2 shows the LDOS for an O ion at the center of the alumina film on Al metal and the position of E_f. Traces of both surface and interface states can be seen near the gap edges, but these would disappear with a thicker film and do not materially effect our conclusions. A thicker film would be more realistic, but computationally more expensive.

Thus atomic H seems the most likely candidate for contributing to electronic conductivity. Where H might reside in the oxide film, and whether the H defect levels will correspond to the electrochemical data, is the subject of the remainder of this paper.

Our bulk DFT calculations for neutral and negative H defects used the local-orbital basis pseudopotential code SEQQUEST.[22] For study of charged defects in supercells, this code uses the local moment counter charge method,[23] a more rigorous treatment of the local Coulomb potential than charge compensation using a uniform (jellium-like) background charge.[16] This code does both LDA and GGA (PBE and PW91) calculations using standard norm-conserving pseudopotentials of both the Hamann[24] (for Al) and Troullier-Martins[25] (for O) type and uses high-quality (double-zeta or better) contracted Gaussian basis sets. Defect calculations were done in 160-atom bulk supercells (four unit cells of κ-Al_2O_3). κ-Al_2O_3 starting atomic coordinates were taken from Ref. 9. Relaxation produced negligible changes. Spin-dependent calculations were used for the paramagnetic neutral H defect. The H^- defect is closed shell and spin polarization unnecessary. With such a large cell, only a single **k** point (at Γ) was needed. Tests with two **k** points show less than a 0.1 eV dispersion in the defect levels, i.e., minimal interaction.

Defect levels with respect to the bulk oxide band edges were located. The slab calculation (above) located these edges with respect to the Al metal E_f. In this way, the relation of the defect levels with respect to E_f could be determined, without the proximity of the slab interface and surface affecting the defect level position.

In κ-Al_2O_3, the largest open region has a central position 1.8 Å from the nearest ion, an O. These voids are the most likely sites for interstitial H. In the relaxed perfect crystal, neutral H was placed in this void, creating a model defect density of 0.6%. The equilibrium H position is a nonbonding site near the center of the void. An H bonded to the nearest O at a distance typical of an O-H bond is not stable in the spin-dependent calculation. Alumina is highly ionic and strongly favors a charge of -2 at the O site; an OH species would reduce this charge to -1. Hence an O-H bond is destabilized and neutral H prefers the center of the void.

The computed bulk oxide band gap is 6.1 eV. The neutral H levels lie 2.2 eV (filled) and 3.5 (empty) above the valence band edge. The oxide E_f is midgap, so this level lies 0.45 eV above E_F. For H^-, the $1s^2$ level lies 3.2 eV above the edge, near the neutral level. This demonstrates an effective screening by the host material. In the H^- defect calculation, the atoms were *not* allowed to relax. The lifetime of an extra conduction electron on the neutral defect is so brief that no motion can occur in the neighboring ions. In Fig. 2, we indicate the approximate energy of the conduction electron, which lies above E_f by roughly 0.2 eV within our model for H^-. It is clear that the filled level in neutral H lies well below E_f while the empty level lies above, indicating an absence of oxidation.

Thus our main theoretical findings are that (1) neutral H is stable in the crystal and in a film on Al(111); (2) the conduction electron energy (making an H^- defect) is above the Al metal E_f by a fraction of an eV, here roughly 0.2 eV; and (3) screening by the oxide reduces the electron-electron repulsion (U) such that tunneling conductivity can occur. In other words, correlation effects do not prevent it. We find remarkable agreement with experiment, especially considering both

the size limitations of the model [a five O-layer film is much thinner than those produced by dry (4 nm) or humid (6 nm) oxidation of clean Al metal[8]] and the well-known band gap problem of DFT.

VASP was developed at the Institut für Theoretische Physik of the Technische Universität Wien. Al thin film sample preparation and H measurement by J. C. Barbour and experimental assistance by R. G. Dunn and R. G. Buchheit are gratefully acknowledged. This work was partly supported by the Department of Energy Office of Basic Energy Sciences (BES). Sandia is a multiprogram laboratory operated by Sandia Corporation, a Lockheed Martin Company, for the United States Department of Energy under Contract No. DE-AC04-94AL85000.

*Email address: drjenni@sandia.gov

[1] M. Gurvitch, M. A. Washington, and H. A. Huggins, Appl. Phys. Lett. **42**, 472 (1983).

[2] J. S. Moodera, L. R. Kinder, T. M. Wong, and R. Meservey, Phys. Rev. Lett. **74**, 3273 (1995).

[3] For example, magnetic random access memory: S. Tehrani, B. Engel, J. M. Slaughter, E. Chen, M. DeHerrera, M. Durlam, P. Naji, R. Whig, J. Janesky, and J. Calder, IEEE Trans. Magn. **36**, 2752 (2000).

[4] D. A. Jones, *Principles and Prevention of Corrosion*, 2nd ed. (Prentice-Hall, Upper Saddle River, NJ, 1996).

[5] W. H. Rippard, A. C. Perrella, F. J. Albert, and R. A. Buhrman, Phys. Rev. Lett. **88**, 046805 (2002).

[6] J. P. Sullivan, J. C. Barbour, R. G. Dunn, K.-A. Son, L. P. Montes, N. Missert, and R. G. Copeland, in *Critical Factors in Localized Corrosion III*, edited by R. G. Kelly, G. S. Frankel, P. M. Natishan, and R. C. Newman (The Electrochemical Society, Pennington, NJ, 1999), p. 111.

[7] J. P. Sullivan, R. G. Dunn, J. C. Barbour, and R. G. Buchheit (unpublished).

[8] B. C. Bunker, G. C. Nelson, K. R. Zavadil, J. C. Barbour, F. D. Wall, J. P. Sullivan, C. F. Windisch, M. H. Engelhardt, and D. R. Baer, J. Phys. Chem. B **106**, 4705 (2002).

[9] Y. Yourdshahyan, C. Ruberto, M. Halvarsson, L. Bengtsson, V. Langer, B. I. Lundqvist, S. Ruppi, and U. Rolander, J. Am. Ceram. Soc. **82**, 1365 (1999).

[10] The effective charges have been estimated at $Al^{+2.8}$ and $O^{-1.8}$: C. Sousa, F. Illas, and G. Pacchioni, J. Chem. Phys. **99**, 6818 (1993).

[11] The gamma phase was not used due to uncertainties in the role of hydrogen. See K. Sohlberg, S. J. Pennycook, and S. T. Pantelides, J. Am. Chem. Soc. **121**, 7493 (1999).

[12] For example, in films of κ-Al_2O_3: D. R. Jennison and A. Bogicevic, Surf. Sci. **464**, 108 (2000).

[13] P. Hohenberg and W. Kohn, Phys. Rev. **136**, B864 (1964); W. Kohn and L. J. Sham, Phys. Rev. **140**, A1133 (1965).

[14] S. M. Sze, *Physics of Semiconductor Devices* (Wiley, New York, 1981).

[15] J. P. Sullivan, K. R. Zavadil, R. G. Dunn, and J. C. Barbour, in *Critical Factors in Localized Corrosion IV*, edited by S. Virtanen, P. Schmuki, and G. S. Frankel (The Electrochemical Society, Pennington, NJ, 2003).

[16] G. Kresse and J. Hafner, Phys. Rev. B **47**, 558 (1993); **49**, 14 251 (1994); **54**, 11 169 (1996).

[17] J. Perdew and A. Zunger, Phys. Rev. B **23**, 5048 (1981); D. M. Ceperley and B. J. Alder, Phys. Rev. Lett. **45**, 566 (1980).

[18] J. P. Perdew, J. A. Chevary, S. H. Vosko, K. A. Jackson, M. R. Pederson, D. J. Singh, and C. Fiolhais, Phys. Rev. B **46**, 6671 (1992).

[19] D. Vanderbilt, Phys. Rev. B **32**, 8412 (1985); **41**, 7892 (1990).

[20] P. J. Eng, T. P. Trainor, G. E. Brown, G. A. Waychvnas, M. Newville, S. R. Sutton, and M. L. Rivers, Science **288**, 1029 (2000), and references therein.

[21] C. Ruberto, Y. Yourdshahyan, and B. I. Lundqvist, Phys. Rev. Lett. **88**, 226101 (2002).

[22] P. A. Schultz (unpublished); for a method description see P. J. Feibelman, Phys. Rev. B **35**, 2626 (1987).

[23] P. A. Schultz, Phys. Rev. Lett. **84**, 1942 (2000).

[24] D. R. Hamann, Phys. Rev. B **40**, 2980 (1989).

[25] N. Troullier and J. L. Martins, Phys. Rev. B **43**, 1993 (1991).